J. Min. Metall. Sect. B-Metall. 59 (2) (2023) 349 - 361

Journal of Mining and Metallurgy, Section B: Metallurgy

EXISTENT STATE AND REMOVAL RATE OF SILVER IN LEAD-SILVER SLAG DURING THE MELT-VAPORIZATION PROCESS

Y.-Y. Shen [a], X.-S. Zhao [a], F.-J. Zhang [a], W.-X. Ma [a], X.-F. Wang [b], X.-Y. Du [a,*]

[a] School of Materials & Science, State Key Laboratory of Advanced Processing and Recycling of Nonferrous Metals, Lanzhou University of Technology, Lanzhou, PR China
[b] Gansu Rare Earth New Material Limited-liability Company, Baiyin, PR China

(Received 19 May 2023; Accepted 02 November 2023)

Abstract

In this paper, Ag contained in the lead-silver slag was recovered during the melt-vaporization process. The existing Ag state in the soot was analyzed, the influence of the reaction temperature, the carbon ratio, and the reaction time on the removal rate of the silver was investigated, and the process conditions were optimized using reaction surface methodology. Silver chloride, silver metal, silver sulfide, silver oxide, and silver sulfate are the main silver phases in lead-silver slag, of which silver chloride and silver sulfide are the main phases. The silver oxide (Ag_2O) and the silver chloride (AgCl) in the lead-silver slag volatilize to soot, the silver sulfide (Ag_2S) is oxidized by oxygen to silver sulfate (Ag_2SO_4), and elemental silver volatilizes with Pb and Zn to form alloys. The silver is ultimately present as Ag, AgCl, Ag_2O and Ag_2SO_4 in the soot. The removal rate of the silver gradually increases with increasing reaction temperature and tends to remain stable at 1300°C. With a gradual increase in the carbon content, the removal rate of silver first increases and then decreases. The highest value is 80.12 wt% when the carbon content is 16.30 wt%. As the holding time increases, the silver removal rate gradually increases and then stabilizes at 79.97 wt% even at a holding time of 150 minutes. The optimum process conditions for silver removal are a reaction temperature of 1340°C, a carbon content of 16.10 wt%, and a holding time of 165 minutes. The average removal rate of silver under these conditions is 80.42 wt%. The research in this article provides a theoretical basis for the removal and utilization of silver from lead and silver residues.

Keywords: *Lead-silver slag; Melt-vaporization process; Silver phase; Response surface method; Removal rate*

1. Introduction

Lead-silver slag is a solid waste produced in hydrometallurgical zinc smelting, and approximately 3000 tons of lead-silver slag is generated for every 10,000 tons of electric zinc produced [1]. The world's greatest zinc metallurgical production in China, more than 6.5 million tons of zinc, has produced large amounts of lead-silver slag simultaneously [2]. Lead-silver slag contains harmful elements such as arsenic, lead, cadmium, copper, and zinc, and the heavy metals in the slag can cause significant harm to human health and environment. It was reported that the concentration of harmful elements in water, soil and plants in areas near smelters is much higher than that in locations far from smelters [3-5]. At present, lead-silver slag is stored in slag fields due to its low reutilization rate, which causes environmental pollution, wastes land resources and makes the recover and reuse of the valuable metals in the slag difficult [6-7]. Therefore, many scholars have investigated methods to recover and extract valuable metals from the slag to recover valuable metals, create economic benefits and protect the environment [8-15]. The melt- vaporization method is based on the fact that the metals (Pb, Zn, Ag, etc.) and metal compounds in the slag have different thermodynamic properties, saturated vapor pressures and melting points and are volatilized into dust during high-temperature treatment. Valuable metals can be recovered from the dust.

The research on roasting metallurgical slag containing Pb and Zn shows that valuable metal resources such as Pb, Zn and Ag can be recovered from flue dust, and metallic iron can be recovered from the slag [16-20]. Wang et al. [21] studied the effects of reaction temperature, reaction time and the pulverized coal ratio on the recovery of lead and zinc in flue gas and the metallization rate of iron in pellets by using a direct reduction method, with jarosite slag as the raw material and pulverized coal as the reducing agent. The optimal experimental conditions were the ratio of pulverized coal of 25 wt%, the temperature of 1250 °C, and the reaction time of 1 h.

Corresponding author: duxy@lut.edu.cn

https://doi.org/10.2298/JMMB230519030S

The recovery rates of lead and zinc were thus 96.97 wt% and 99.89 wt%, respectively. Li et al. [22] used the method of reduction roasting to study the effects of coke addition, temperature, reaction time and CaO addition on the recovery of metal zinc and metal lead from dust in lead-silver slag, and the optimum process conditions were roasting at a constant temperature, a coke dose of 40 wt%, a temperature of 1200 ℃, a reaction time of 1 h and a CaO additive dose of 4 wt%., the volatilization rates of zinc and lead were 98.85 wt% and 97.6 wt%, respectively. Xu et al. [23] used oxygen bottom-blowing smelting to synergistically treat lead-silver slag, and the results showed that the process could be used to recover 98 wt% lead, 90 wt% zinc, and 98.5 wt% silver from the flue dust and slag.

Ag is a precious transition metal present in lead-silver slag, with a content of approximately 150.00 g/t. The melt-vaporization process has a large treatment capacity and high treatment efficiency, resulting in a high recovery of lead, zinc and silver. However, during the melt-vaporization process, the phase evolution and state of Ag volatilized from the lead-silver slag is unclear. Therefore, in this paper, the melt-vaporization method was used to treat lead-silver slag, and the phase evolution of silver in the treatment process was studied. The influence of reaction temperature, the carbon ratio, and holding time on the removal rate of silver was explored, and the response surface method was used to analyze the optimal process parameters for silver removal, which provided a theoretical basis for the comprehensive recovery of silver from lead-silver slag.

2. Experiment

2.1. Experimental materials

The raw material used in this paper was lead-silver slag from the Northwest Lead-Zinc Smelter of Baiyin Nonferrous Group Co., Ltd. After being dried at 80 ℃ for 24 h, the slag samples with particle sizes less than 0.074 μm were broken and sieved through a 200 mesh sieve. The chemical composition of the lead-silver slag was analyzed by inductively coupled plasma spectrometry (ICP, ICAP-7000, Thermo Fisher), and the results are shown in Table 1. Table 1 shows that the content of Ag in the lead-silver slag was 149.00 g/t.

The results from X-ray diffraction (XRD, Rigaku D/max-2004, Rigaku) analysis of the lead-silver slag are shown in Figure 1 (a). The main phases in the lead-silver slag were jarosite ($KFe_3(SO_4)_2(OH)_6$), quartz (SiO_2), zinc sulfate ($ZnSO_4$), iron oxide (Fe_2O_3), lead sulfate ($PbSO_4$) and zinc ferrite ($ZnFe_2O_4$).

Due to the low content of silver, the silver-containing phase cannot be detected. The microstructure and main elemental distribution of the

Table 1. *Composition analysis of the lead-silver slag (wt%)*

Element	Fe	Zn	Pb	Sb	Ag*	Ca	S
Content/wt%	20.3	6.43	3.66	0.13	149	5.23	14.03
Element	Al	Cd	As	Si	Ga*	In*	Ge*
Content/wt%	0.86	0.14	0.19	6.02	13.9	44	8.5

*Note: * indicates g/t*

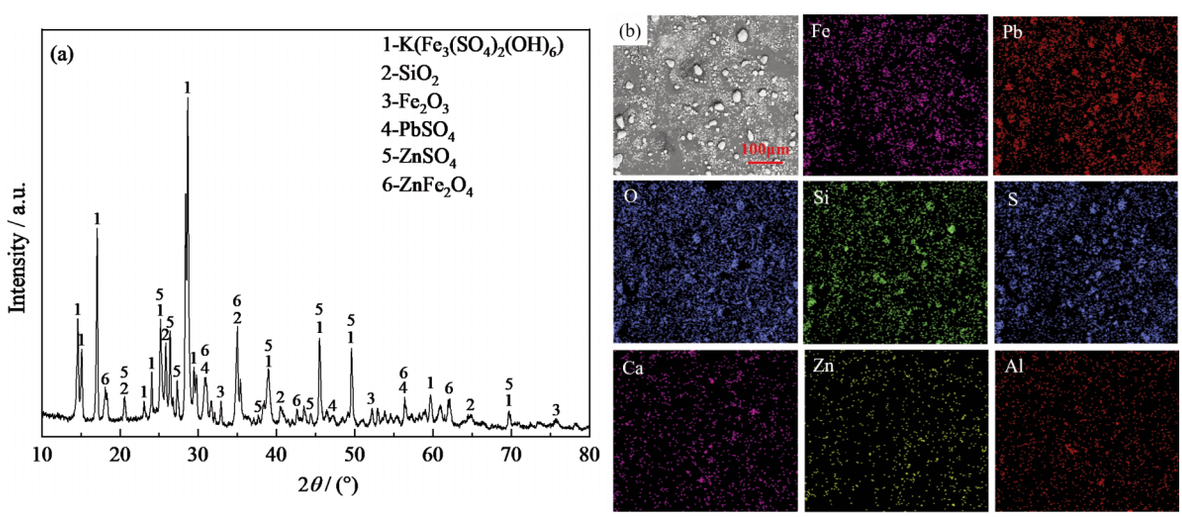

Figure 1. *(a) XRD spectra of the lead-silver slag; (b) SEM diagram of the lead-silver slag and surface scanning diagram of different elements*

lead-silver slag were analyzed by scanning electron microscopy (SEM, JSM-6700F, JEOL), as shown in Fig. 1(b). It can be seen from the surface scanning energy spectrum that Fe, Pb, O, Si, S, Ca and Zn were mainly distributed in the lead-silver slag and consisted of large particles, and Al was evenly distributed.

Chemical phase analysis of silver in the lead-silver slag was carried out, and the results are shown in Table 2. Silver chloride, metallic silver, silver sulfide, silver oxide and silver sulfate were the main phases of silver in the lead-silver slag, among which the contents of silver chloride and silver sulfide were much higher than that of metallic silver and silver oxide and silver sulfate. Additionally, Ag was associated with Pb, Zn and other elements in the lead-silver slag [24-26].

In this experiment, carbonaceous material was used as the reducing agent, and the carbon powder was obtained from the Northwest Lead-Zinc Smelter of Baiyin Nonferrous Metals Group Co., Ltd. The results from the analysis of the carbon powder are shown in Table 3.

2.2. Experimental method

The lead-silver slag was pretreated, and the original slag was dried in a vacuum drying oven (DZF-6030A, Yiheng) at 80 °C for 24 h. After drying, the lead-silver slag was loaded into a style crusher (GJ-400-1, Yongsheng) for crushing and was sieved through a 200 mesh screen.

The pretreated lead-silver slag was mixed with a certain proportion of carbon powder, placed into a ball mill (QM-3SP04, Nju-instrument), mixed thoroughly, dried after mixing and then pressed into flakes using a tablet press (FW-4, Tjtp) at a pressure of 20 MPa. The slag sample was placed in a corundum crucible, and the total mass of the corundum crucible and the slag sample was weighed.

The slag sample was placed into a high-temperature dust collection furnace (KSL-1700X-A2, Kjmti), and the corresponding reaction temperature and holding time were set. A fan was used to inject air into the stove, and the gas flow rate was 600 mL/min. The condensation dust collection device was turned on, and the furnace was closed after the temperature of the furnace dropped to room temperature.

The soot in the dust collection box and the exhaust pipe were collected and uniformly mixed, and the phase and microstructure of silver in the soot were analyzed. The corundum crucible was removed from the furnace and its total weight was measured, and the corundum crucible was crushed to collect the tailings after the experiment, which were destroyed by a crusher and screened by a 200 mesh sieve. The silver content in the tailings was measured, and the removal rate of silver in the lead-silver slag was calculated according to Formula (1).

$$R = \frac{m_s \cdot w_1 - m_T \cdot w_2}{m_s \cdot w_1} \cdot 100\% \quad (1)$$

where R is the removal rate of silver, wt%; m_s is the mass of lead-silver slag, g; w_1 is the content of metal zinc in lead-silver slag, wt%; m_T is the mass of tailings after the lead-silver slag reaction, g; and w_2 is the content of metallic silver in the tailings after the lead-silver slag reaction, wt%.

Since the content of silver in lead-silver slag was only 149.00 g/t, the phase and microstructure of the silver were difficult to characterize. Therefore, an expanded slag batch experiment with high silver content was carried out. Table 2 shows that the silver phases in the lead-silver slag were mainly Ag_2S and AgCl, together accounting for 93.15 wt%. Therefore, Ag_2S and AgCl were added to the original slag for the experiment. The additional Ag_2S added (analytically pure, Shanghai Macklin Biochemical Technology Development Co., Ltd.) was 5.85 wt%, and the additional AgCl added (analytically pure, Shanghai Macklin Biochemical Technology Development Co., Ltd.) was 3.46 wt%. A certain proportion lead and silver slag, carbon powder, Ag_2S and AgCl was pretreated via ball milling to mix evenly and was then dried. The samples were placed in a corundum crucible in a high-temperature dust collection furnace, and soot and slag were collected. XRD phase analysis was performed on the soot, SEM-EDS characterization methods were used to observe the microstructure of the soot, and the mineral states were analyzed by mineral dissociation analysis (MLA, V2.7, FEI). The phase and content of Ag in the slag and soot were determined by chemical phase analysis

Table 2. *Results of silver phase analysis in the lead-silver slag*

Phase	AgCl	Ag	Ag_2S	Ag_2O	Ag_2SO_4	Footing
Occupation/g, t-1	51.60	5.30	87.20	1.40	3.50	149.00
Occupation rate/wt%	34.63	3.56	58.52	0.94	2.35	100.00

Table 3. *Carbon powder composition analysis*

Component	Ash					Volatile	Fixed carbon	Total sulfur
	Fe	CaO	MgO	Al_2O_3	SiO_2			
Content/wt%	1.14	0.91	0.10	3.43	5.73	2.06	83.07	0.72

and ICP, and the removal rate of silver was calculated based on theoretical calculations and experimental results.

Optimized single-factor experimental conditions were selected to study the effect of experimental conditions on the silver removal rate in the lead-silver slag. In Design Expert, the response surface method module based on the Box-Behnken Design was used to optimize the silver removal rate, and then the response surface model was fitted and analyzed. Finally, the response surface experimental design was implemented and optimized to verify the results. In this paper, a response surface experimental design consisting of three factors and three levels was adopted. The three levels were denoted by -1, 0, and 1. The reaction temperature (A), carbon ratio (B), and holding time (C) were independent variables, and the silver removal rate (R_{Ag}) was used as the response value for experimental optimization.

3. Results and discussion

3.1. Thermomechanical analysis

The Gibbs free energy of the silver phase in the lead-silver slag during the melt-vaporization process was calculated by the reaction module in the thermodynamic software FactSage. Table 2 shows that the silver phases in the lead-silver slag were silver chloride (AgCl), silver sulfide (Ag_2S), silver oxide (Ag_2O) and silver sulfate (Ag_2SO_4). The chemical reactions that may occur during the melt-vaporization process were as follows:

$$2Ag_2S + C = 4Ag + CS_2 \quad (2)$$

$$Ag_2S + CO = 2Ag + COS \quad (3)$$

$$1/2Ag_2SO_4 + C = Ag + 1/2SO_2 + CO \quad (4)$$

$$1/2Ag_2SO_4 + CO = Ag + 1/2SO_2 + CO_2 \quad (5)$$

$$Ag_2O + C = 2Ag + CO \quad (6)$$

$$Ag_2O + CO = 2Ag + CO_2 \quad (7)$$

$$1/2Ag_2S + O_2 = 1/2Ag_2SO_4 \quad (8)$$

The Gibbs free energy of the above reactions (2)-(8) in the temperature range 0-1500 °C at standard atmospheric pressure was calculated. Fig. 2(a) shows the relationship between different reactions ΔG^{θ} and the temperature of the silver phase. It can be seen from the figure that Ag_2S could not be reduced by carbon and carbon monoxide, while Ag_2S could be oxidized by oxygen oxidation to form Ag_2SO_4. Ag_2O and Ag_2SO_4 could react with carbon and carbon monoxide, but Ag_2SO_4 did not react with carbon when the temperature was less than 100 °C.

The possible decomposition reactions of the four phases (AgCl, Ag_2S, Ag_2O and Ag_2SO_4) of silver in the lead-silver slag were as follows:

$$AgCl = Ag + 1/2Cl_2 \quad (9)$$

$$1/2Ag_2SO_4 = Ag + 1/2SO_2 + 1/2O_2 \quad (10)$$

$$1/2Ag_2S = Ag + 1/4S_2 \quad (11)$$

$$1/2Ag_2O = Ag + 1/4O_2 \quad (12)$$

Fig. 2(b) shows the relationship between ΔG^{θ} and the temperature of the silver phase decomposition reaction. As seen from the figure, AgCl and Ag_2S did not decompose. When the temperature exceeds 200 °C, decomposition of Ag_2O tended to occur. When the temperature was 1300 °C, Ag_2SO_4 tended to decompose.

The Equilib module was used to calculate the vapor pressure of the silver phase in the thermodynamic software FactSage. The relationship between the vapor pressure of the silver phase and the temperature is shown in Fig. 2(c). It can be seen from the figure that Ag_2O had a high vapor pressure at a temperature of 200 °C, indicating that Ag_2O had good volatility and volatilized into the flue gas. When the temperature reached 600 °C, the vapor pressure of Ag_2SO_4 began to increase and increased sharply after a temperature of 900 °C was reached. Combined with the reaction Gibbs free energy, the results show that Ag_2SO_4 was preferentially reduced to metallic silver at low temperatures, and volatilization was preferred to reduction at higher temperatures. When the temperature was 1000 °C, the vapor pressure of AgCl gradually increased, reaching its maximum at more than 1300 °C, at which point AgCl volatilized into the soot. The vapor pressure of Ag_2S and Ag was low at 1200-1600 °C, indicating that Ag_2S and Ag did not have volatile properties at the experimental temperature.

3.2. State of Ag in soot

The XRD physical phase analysis of the soot collected from the silver slag experiment is shown in Fig. 3(a), which presents the XRD spectrum of the silver slag soot. Based on the results in Fig. 3(a), the main phases of the soot were ZnO, PbS, PbO, AgCl, Ag_2O and Ag_2SO_4, in which silver existed in the form of AgCl, Ag_2O and Ag_2SO_4.

SEM-EDS analysis was conducted on the soot collected from the silver slag experiment. In Fig. 3(b), the dense distribution area of Ag was consistent with that of Cl. The atomic ratio of Ag to Cl was close to 1:1, suggesting the presence of AgCl. The atomic ratio

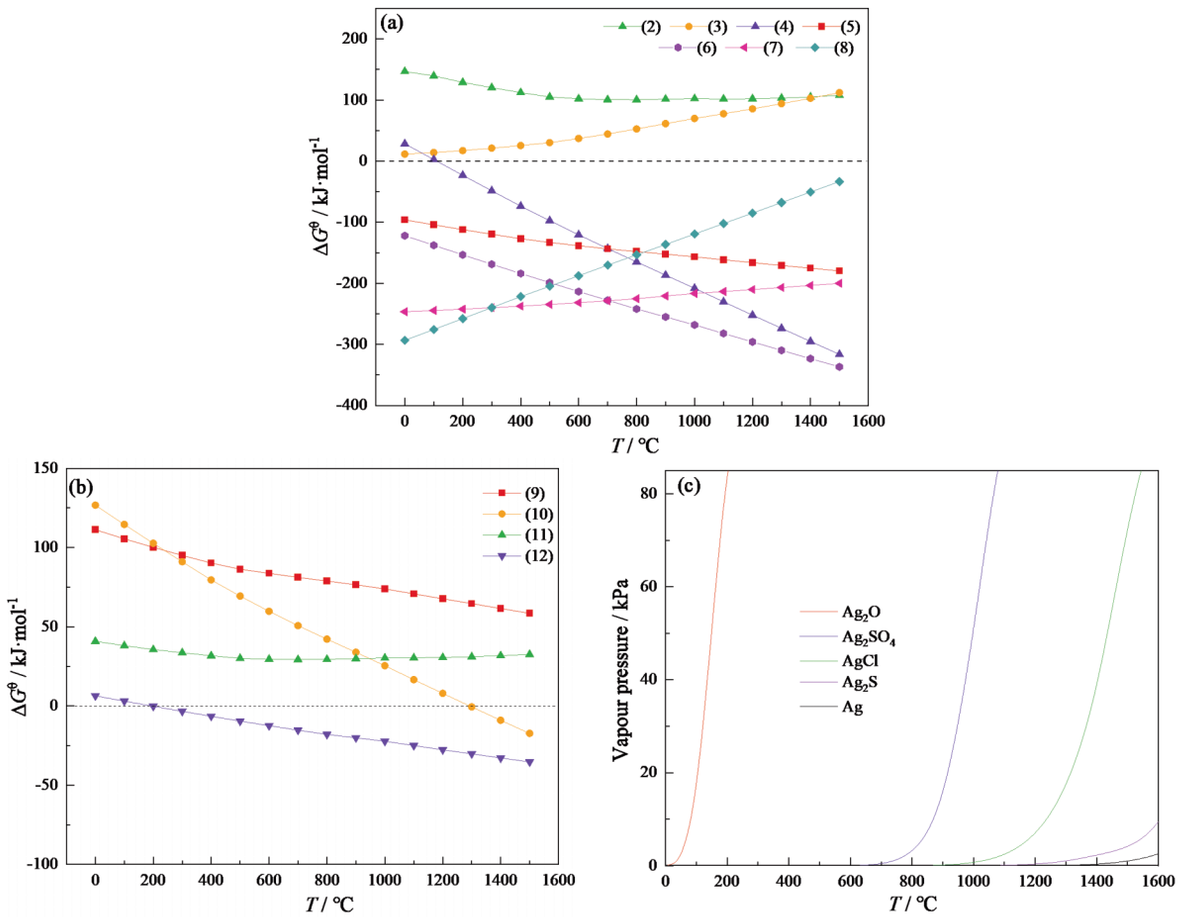

Figure 2. *(a) Relationship between different reaction ΔG^{θ} values of the silver phase and temperature. (b) The relationship between the silver phase decomposition reaction ΔG^{θ} and temperature. (c) The relationship between vapor pressure and temperature of the silver phase*

of Zn to O in the rod-like material was close to 1:1, indicating the existence of ZnO.

Fig. 3(c) is the SEM-EDS spectrum of Ag_2O in the soot. It can be seen from the diagram that Ag was distributed in gray–white area 1, and Pb was distributed in dark gray area 2, which was complementary to the location where Ag was located. O, Zn, S and Cl existed simultaneously. It can be seen from Fig. 1 that the atomic ratio of Ag to O in the gray area was approximately 2:1. The analysis of XRD and surface scan of the soot imply that Ag_2O existed in the soot.

Fig. 3(d) is the SEM-EDS spectrum of Ag_2SO_4. It can be seen from the figure that the dense distribution of Ag in region 1 was consistent with that of S. O was enriched in the whole region, and the atomic ratio of Ag to O to S was approximately 2:4:1 according to spectrum 1. Comprehensive analysis of the XRD data and the surface scan of the soot showed that soot area 1 was Ag_2SO_4. Region 2 was rich in Zn and O. In area 2, the atomic ratio of Zn to O was approximately 1:1, and soot region 2 was ZnO.

Fig. 4 shows the backscattered electron micrographs of soot MLA. As seen from Fig. 4(a), the silver-lead alloy showed that most silver-bearing minerals in the ore sample were entirely or partially encapsulated with lead due to the intergrowth of silver minerals and carrier minerals. It can be seen from Fig. 4(b) that the silver minerals in the zinc-silver alloy were distributed in a wrapped or connected state with metallic zinc and zinc oxide. Monolithic silver was mainly formed as a Pb-Zn alloy and carried into the soot by Pb and Zn volatilization.

3.3. Effects of reaction temperature, the carbon ratio and holding time on the silver removal rate

Based on the melting characteristics and thermodynamic calculations of the lead-silver slag, the effect of reaction temperature on silver removal in the range of 1100-1400 °C was studied. Fig. 5(a) shows the effect of reaction temperature on the removal rate of silver in lead-silver slag under experimental conditions consisting of a holding time of 120 min and a

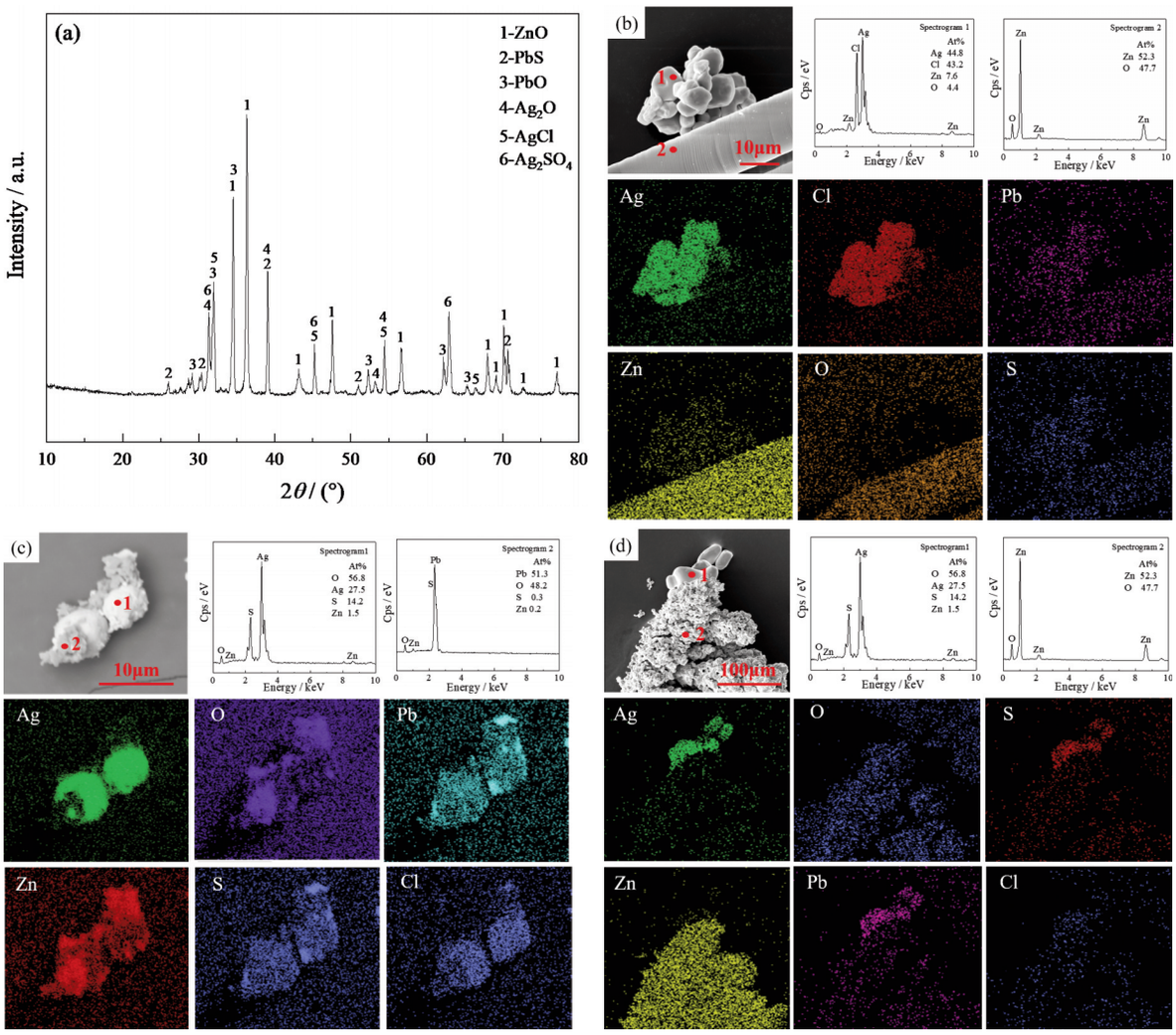

Figure 3. *(a) XRD spectrum of soot; SEM-EDS spectra of different phases in soot: (b) AgCl, (c) Ag_2O, (d) Ag_2SO_4*

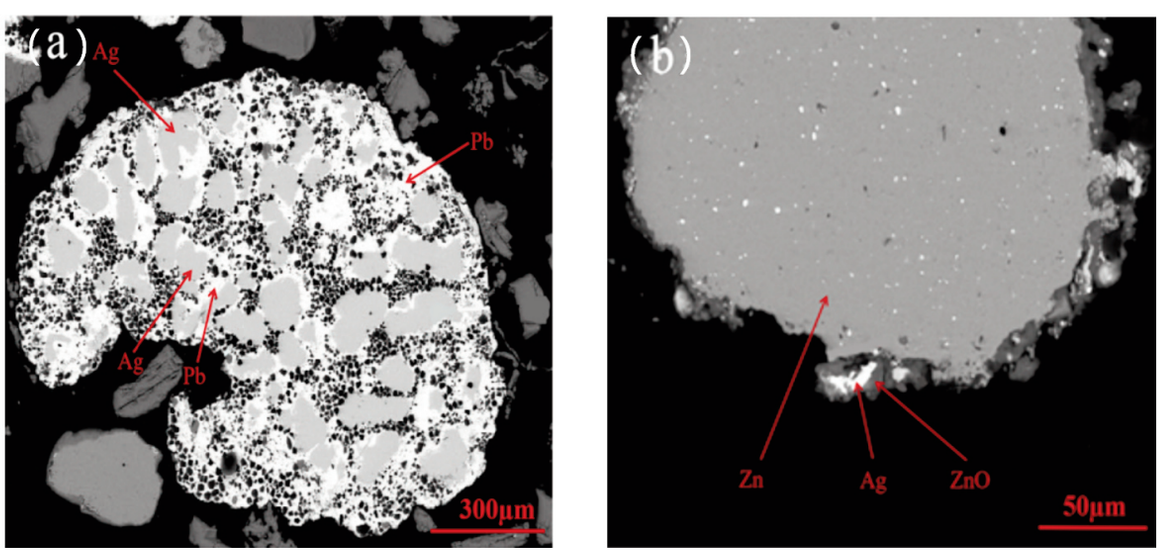

Figure 4. *MLA backscattered electron microscopy images of soot*

theoretical carbon ratio of 14.30 wt%. As seen in the figure, silver removal from the lead-silver slag in the melt-vaporization process gradually increased with increasing reaction temperature. It tended to stabilize at 1300 °C because the reaction proceeded more fully with an increase in reaction temperature. When the reaction temperature was 1100 °C, the removal rate of silver was only 24.01 wt% because the lead-silver slag was not entirely melted at the lower reaction temperature, and contact between the materials is insufficient. The vapor pressure of AgCl increased slowly at this reaction temperature. When the reaction temperature rose to 1300 °C, the removal rate of silver increased to 80.26 wt%. The silver in the soot was mainly AgCl, Ag_2SO_4, metallic silver in the form of alloys and Ag_2O. When the reaction temperature exceeded 1300 °C, the removal rate of silver remained unchanged. The highest removal rate of silver was 81.29 wt% at 1400 °C. Considering comprehensive energy consumption, a reaction temperature of 1300 °C was selected as the best temperature for silver removal.

Fig. 5(b) shows the experimental results of the effect of the carbon ratio on the removal rate of silver in the lead-silver slag under experimental conditions consisting of a reaction temperature of 1300 °C and a holding time of 120 min. It can be seen from the figure that during the melt-vaporization process of the lead-silver slag, the removal rate of silver increased first and then decreased with a gradual increase in the carbon ratio. When the carbon ratio was 10.30 wt%, the silver removal was only 61.54 wt%. The amount of carbon powder added was insufficient, the reducing atmosphere was weak, and the volatilization rate of lead and zinc was low. The highest removal rate of silver was 80.12 wt% when the carbon ratio was 16.30 wt%. When the carbon ratio increased to 22.30 wt%, the removal rate of silver was 76.13 wt%. The reason for the decrease in removal was that when an excessive amount of carbon powder was added, some of the carbon did not burn sufficiently to accumulate in the slag, making the slag less fluid and more viscous, which affected the volatilization of lead and zinc, decreasing silver removal [27-28]. Based on the above considerations and comprehensive analysis, it was concluded that a final carbon allocation ratio of 16.30 wt% was best for silver removal.

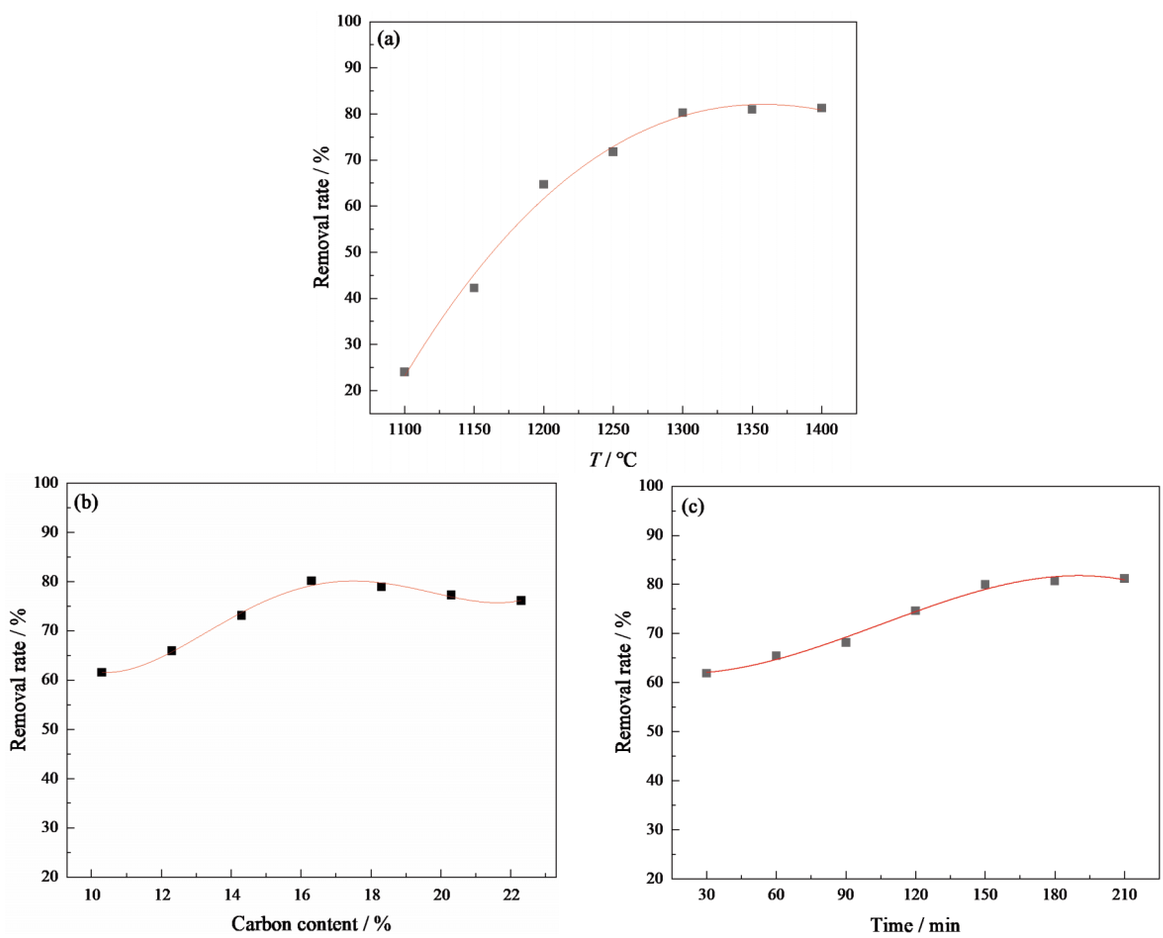

Figure 5. *Silver removal under different reaction conditions: (a) reaction temperature, (b) carbon ratio, and (c) holding time*

Fig. 5(c) shows the effect of holding time on the removal rate of silver in the lead-silver slag under experimental conditions consisted of a reaction temperature of 1300 ℃ and a carbon ratio of 16.30 wt%. It can be seen from the figure that the removal rate of silver in the melt-vaporization process of lead-silver slag gradually increased with increasing holding time and then tendsed to be stable. When the holding time was 30 min, the removal rate of silver was only 61.90 wt%. As the holding time increased to 150 min, the removal rate of silver was 79.97 wt%. A sufficient holding time was conducive to the volatilization of AgCl and Ag_2SO_4 and the reaction of lead and zinc, so the removal rate of silver increased with increasing holding time. When the holding time was increased to 210 min, the highest silver removal rate was 81.18 wt%. When the holding time was increased to more than 150 min, the reaction of silver reached equilibrium, and the removal rate did not change with increasing holding time. Hence, the silver removal rate tended to be stable. To achieve best silver removal, a holding time of 150 min was chosen based on considerations of comprehensive energy consumption and production efficiency.

3.4. Optimization of process conditions by the response surface methodology

Based on the single-factor experimental results, the Box–Behnken Design module in Design-Expert10.0 software was used to design experiments. Reaction conditions were optimized with reaction temperature (A), carbon ratio (B) and holding time (C) as independent variables and the silver removal rate (R_{Ag}) as the response value. Table 4 shows the experimental design for three factors and three levels. The response surface experimental design and results are shown in Table 5.

The experimental data for silver removal in Table 5 were fitted with multiple regression analysis, and the multiple regression equation for silver removal from lead-silver slag based on the reaction temperature, carbon ratio and holding time is shown in (13).

$$R_{Ag} = 80.00 + 4.18A + 2.98B + 2.48C + 0.19AB - 0.89AC - 0.015BC - 3.59A^2 - 3.98B^2 - 1.80C^2 \quad (13)$$

In the formula, R_{Ag} represents the removal rate of silver (wt%), A represents the reaction temperature (°C), B represents the carbon ratio (wt%), and C represents the holding time (min). From the Formula (13) multiple regression equation, the order of influence of individual factors on the silver removal rate is A > B > C. Table 6 shows the results of regression analysis of variance.

As seen in Table 6, the *F* value of the silver removal rate in the model was 224.98, indicating that this model was significant in predicting the experimental results. The *F* value of the mismatch term was 3.29, and this model's P value was significant in predicting the experimental results, at 0.1402 (P<0.05 was considered significant), indicating that the regression model fitted well. Based on the *F* value and *P* value in the multiple regression equation and variance analysis of the regression equation, it can be seen that reaction temperature and holding time had a significant effect on the removal rate of silver. The order of influence of the three individual factors on the removal rate of silver is A>B>C, that is, the reaction temperature>carbon ratio>holding time, and the order of the square of the three individual factors on the removal rate of silver was B^2> A^2>C^2. The results of the statistical analysis of the regression equation errors are shown in Table 7.

The model R^2=0.9966, which meant that the accuracy of the experimental results was 99.66 wt%;

Table 4. *Factors and level conditions*

Level	A: Reaction temperature/ ℃	B: Carbon ratio/wt%	C: Holding time/min
-1	1250	14.30	120
0	1300	16.30	150
1	1350	18.30	180

Table 5. *Response surface experimental design and results*

Experiment sequence	A: Reaction temperature /℃	B: Carbon ratio/wt%	C: Holding time/min	RAg: Silver removal/wt %
1	1300	18.30	120	74.65
2	1300	16.30	150	80.18
3	1250	16.30	180	73.34
4	1350	18.30	150	79.42
5	1300	16.30	150	80.23
6	1250	14.30	150	65.83
7	1300	16.30	150	80.15
8	1300	16.30	150	79.98
9	1350	16.30	120	77.66
10	1300	14.30	120	68.58
11	1350	14.30	150	73.15
12	1300	16.30	150	79.45
13	1300	14.30	180	73.82
14	1250	16.30	120	66.86
15	1250	18.30	150	71.34
16	1300	18.30	180	79.83
17	1350	16.30	180	80.58

CV=0.60%<10%, indicating that the model was accurate and credible; in this model, Adj R^2=0.9921, Pred R^2=0.9592, R_{Adj}^2- R_{Pred}^2=0.0329<0.2, indicating that the silver removal model fits the actual data well [29].

Through analysis and calculation in the Design-Expert software, the residual normal distribution for the silver removal rate model (Fig. 6(a)) and the predicted value and actual value distribution (Fig. 6(b)) were obtained. As seen in the figure, the residual average distribution data points were distributed on both sides of a straight line, and most of their values fell between -2 and 2. The predicted and actual values basically fell on a straight line, indicating that the model to fit the silver removal rate based on the response surface methodology had good adaptability.

Fig. 7 shows the three-dimensional response surface diagram and contour map of the effect of reaction temperature and the carbon ratio, reaction temperature and holding time, and the carbon ratio

Table 6. *Variance analysis of the regression equation*

	Quadratic sum	Degrees of freedom	Mean square	F Ratio	P Ratio	Significance
Model	411.68	9	45.74	224.98	< 0.0001	Predominance
A	139.78	1	139.78	687.51	< 0.0001	Predominance
B	71.16	1	71.16	350.02	< 0.0001	Predominance
C	49.1	1	49.1	241.52	< 0.0001	Predominance
AB	0.14	1	0.14	0.71	0.4272	Nonsignificant
AC	3.17	1	3.17	15.6	0.0055	Predominance
BC	0.0009	1	0.0009	0.00443	0.9488	Nonsignificant
A2	54.16	1	54.16	266.39	< 0.0001	Predominance
B2	66.58	1	66.58	327.47	< 0.0001	Predominance
C2	13.66	1	13.66	67.21	< 0.0001	Predominance
Residual error	1.42	7	0.2			
Misfit term	1.01	3	0.34	3.29	0.1402	Nonsignificant
Pure error	0.41	4	0.1			

Table 7. *Statistical analysis of regression equation error*

Statistical project	Value	Statistical project	Value
Std. Dev.	0.45	R-Squared	0.9966
Mean	75.59	Adj R-Squared	0.9921
CV wt%	0.60	Pred R-Squared	0.9592
PRESS	16.84	Adeq Precision	43.129

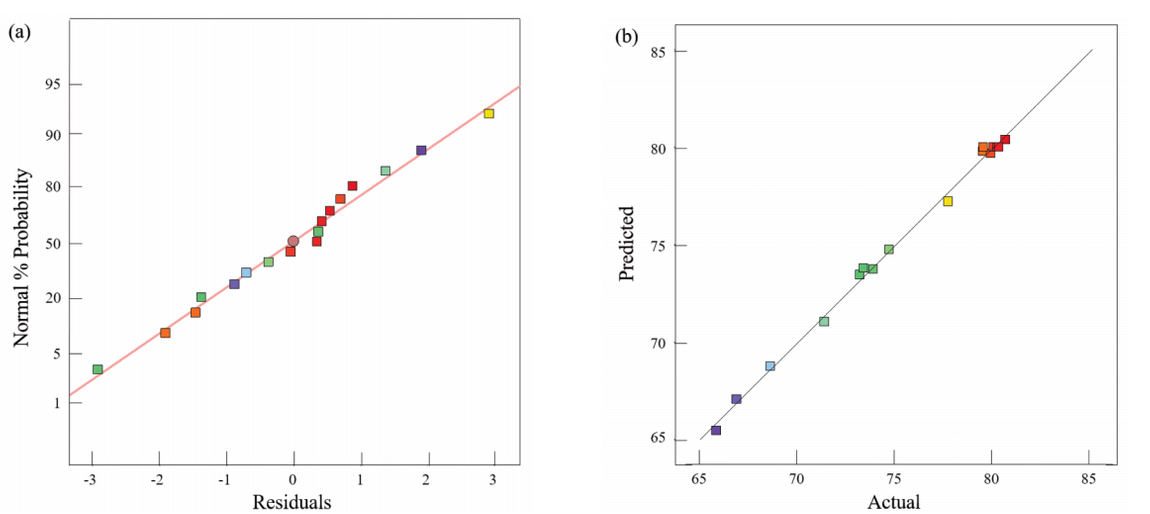

Figure 6. *(a) Residual normal distribution diagram; (b) distribution of predicted and actual values*

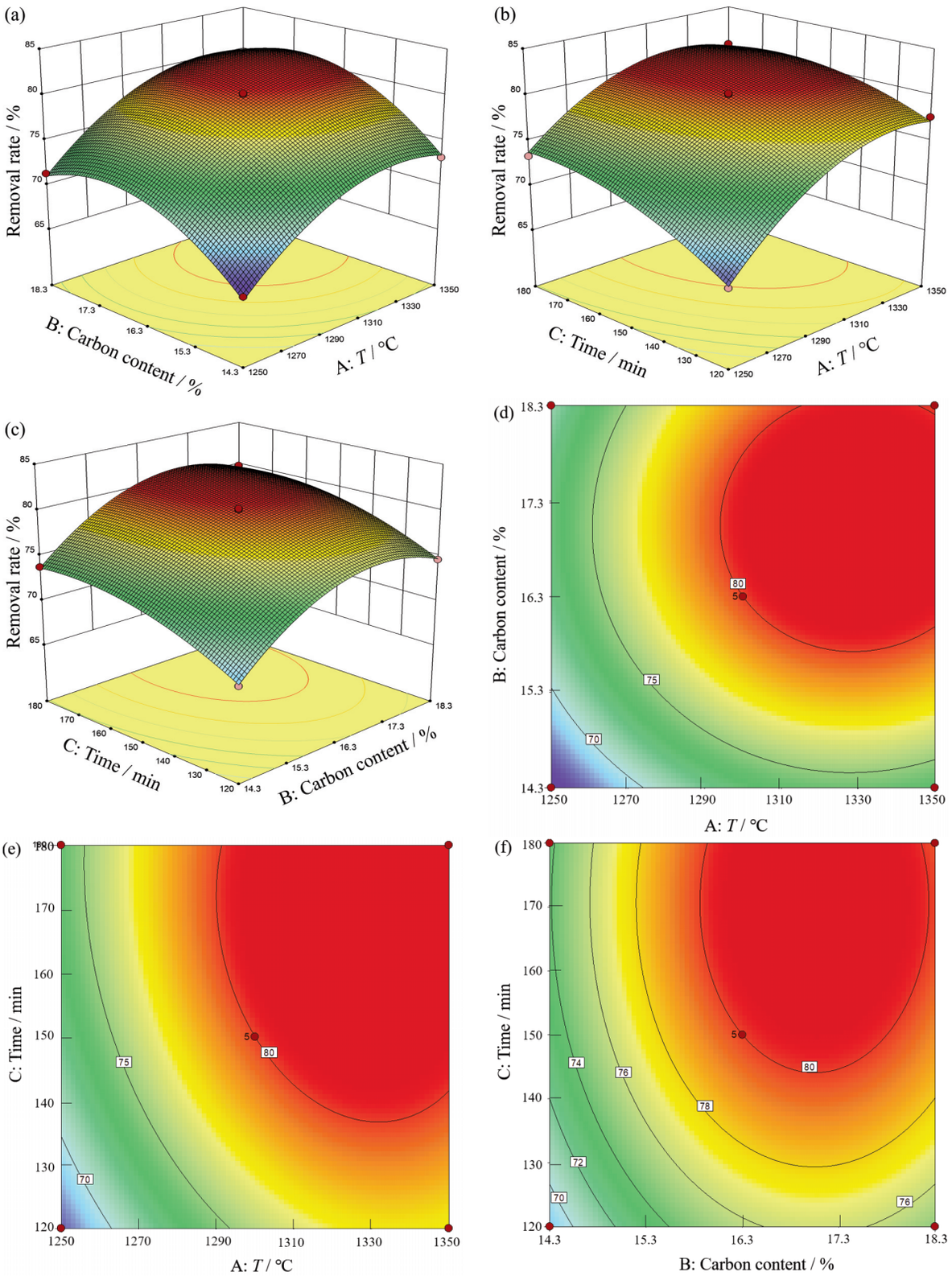

Figure 7. *Response surface plots and contour map of the effects of different reaction conditions on silver removal: (a) and (d) reaction temperature and carbon ratio, (b) and (e) reaction temperature and holding time, (c) and (f) carbon ratio and holding time*

and holding time on the silver removal rate.

From the analysis of the three-dimensional response surface plots of silver removal in Fig. 7, it is clear that there was an optimal interval for silver removal when the reaction temperature was in the range of 1290-1350 ℃, the carbon ratio was between 15.30 wt% and 17.30 wt%, and the holding time was in the range of 140-180 min. These three factors significantly affected the silver removal rate, and they were ranked in order from most significant to least significant as reaction temperature, carbon ratio, and holding time. It can be seen from the contour map analysis that the shape of the contour map between the reaction temperature and the carbon ratio (AB) was close to a circle, indicating that the interaction between the reaction temperature and the carbon ratio had no significant effect on the silver removal rate. The shapes of the contour maps of reaction temperature and holding time (AC) and the carbon ratio and holding time (BC) were close to ellipses, and the interaction between them significantly affected silver removal.

According to the predicted results of the model, the optimum conditions for silver removal were obtained: the reaction temperature was 1339.88 ℃, the carbon ratio was 16.13 wt%, and the holding time was 165.27 min. Combined with the comprehensive analysis, the optimal conditions for adjusting the silver removal rate were as follows: the reaction temperature was 1340 ℃, the carbon ratio was 16.10 wt%, and the holding time was 165 min. Three experiments were carried out to verify the optimal process. The average silver removal rate was 80.42 wt%, which was close to the predicted results. These findings have particular research significance for extracting metallic silver from lead-silver slag.

4. Conclusion

1) The content of Ag in the lead-silver slag was 149.00 g/t. Silver chloride, metallic silver, silver sulfide, silver oxide and silver sulfate were the main phases of silver in the slag, and the contents of silver chloride and silver sulfide were higher than that of other silver phases.

2) Ag_2O and silver AgCl in the lead-silver slag volatilize into dust, Ag_2S was oxidized by oxygen to generate (Ag_2SO_4), and Ag, Pb, and Zn form an alloy and volatilize. The composition of the final soot consisted of the minerals ZnO, PbS, PbO and elemental silver, as well as AgCl, Ag_2O and Ag_2SO_4, while the forms of silver in the soot were Ag, AgCl, Ag_2O and Ag_2SO_4.

3) The removal rate of silver in the melt-vaporization process gradually increased with increasing reaction temperature and tended to remain stable at 1300 ℃. At 1300 ℃, the removal rate of silver rose to 80.26 wt%. With an increase in the carbon ratio, the removal rate of silver first increased and then decreased. When the carbon ratio was16.30 wt%, the removal rate of silver reached its highest value, which was 80.12 wt%. The removal rate of silver was 79.97 wt% when the holding time increased to 150 min. The optimal process conditions for silver removal were a reaction temperature of 1340 ℃, a carbon ratio of 16.10 wt% and a holding time of 165 min. The average silver removal rate reached 80.42 wt%.

Acknowledgments

This work was financially supported by the National Natural Science Foundation (No. 52164034), the Baiyin-City Science and Technology "Unveiling List" System Project (2022-2J), the Gansu Provincial Science and Technology Commissioner Special (22CX8GA123), the Science and Technology Major Project Plan of Gansu Province Grant Nos. (19ZD2GD001, 22ZD6GA008) and the National Natural Science Foundation of China (U22A20175).

Author contributions

Writing-original draft, investigation, data curation: Xianshao Zhao. Conceptualization, Funding acquisition, Writing-review & editing: Yingying Shen. Supervision: Xueyan Du. Investigation: Fengji Zhang and Weixing Ma. Validation: Xinfeng Wang.

Data availability

The data used to support the findings of this study are available from the corresponding author upon request.

Conflict of Interest

The authors declare no competing financial interests.

Reference

[1] Y. Y. Wang, Y. L. Yuan, G. Y. Wen, R. X. Wang, Comprehensive recovery of valuable metals from lead-silver residue using low-temperature alkaline smelting, Transactions of the Indian Institute of Metals, 74 (12) (2021) 3013-3023. http://doi.org/10.1007/s12666-021-02310-w.

[2] Z. G. Pan, P. Xia, Q. Zhu, T. Long, J. Han, H. W. Wu, P. P. Liu, X. H. Zhang, Analysis on development and utilization of zinc resources in China, Acta Geoscientica Sinica, 42 (2) (2021) 258-264. (In Chinese)

[3] R. T. Wilkin, T. R. Lee, D. G. Beak, R. Anderson, B. Burns, Groundwater co-contaminant behavior of

arsenic and selenium at a lead and zinc smelting facility, Applied Geochemistry, 89 (2018). 255-264. http://doi.org/10.1016/j.apgeochem.2017.12.011.

[4] Y. P. He, Z. W. Han, F. Z. Wu, J. Xiong, S. Y. Gu, P. Wu, Spatial distribution and environmental risk of arsenic and antimony in soil around an antimony smelter of qinglong county, Bulletin of Environmental Contamination and Toxicology, 107 (6) (2021) 1043-052. http://doi.org/10.1007/s00128-021-03118-6.

[5] T. Zhou, Z. Y. Wang, P. Christie, L. H. Wu, Cadmium and lead pollution characteristics of soils, vegetables and human hair around an open-cast lead-zinc mine, Bulletin of Environmental Contamination and Toxicology, 107 (6) (2021) 1176-1183. http://doi.org/10.1007/s00128-021-03134-6.

[6] S. L. Wang, X. Gao, Q. Zhao, C. H. Yue, R. S. Su, J. J. Si, X. Q. Ma, Study on the extraction process of various elements in lead-silver slag, Modern Chemical Industry, 35 (1) (2015) 80-83. (In Chinese) http://doi.org/10.16606/j.cnki.issn0253-4320.2015.01.032.

[7] R. X. Wang, Y. D. Yang, C. X. Liu, J. Zhou, Z. Fang, K. Yan, L. Tian, Z. F. Xu, Recovery of lead and silver from zinc acid-leaching residue via a sulfation roasting and oxygen-rich chlorination leaching method, Journal of Central South University, 27 (2020) 3567-3580. http://doi.org/10.1007/s11771-020-4569-6.

[8] A. Akcil, Y. A. Lbrahim, P. Meshram, S. Panda, Hydrometallurgical recycling strategies for recovery of rare earth elements from consumer electronic scraps: a review, Journal of Chemical Technology and Biotechnology, 96 (7) (2021) 1785-1797. http://doi.org/10.1002/jctb.6739.

[9] S. Javanshir, S. S. Qashoqchi, Z. H. Mofrad, Silver production from spent zinc-silver oxide batteries via leaching-cementation technique, Separation Science and Technology, 56 (11) (2021) 1956-1964. http://doi.org/10.1080/01496395.2020.1797800.

[10] P. Xing, B. Z. Ma, P. Zeng, C. Y. Wang, L. Wang, Y. L. Zhang, Y. Q. Chen, S. Wang, Q. Y. Wang, Deep cleaning of a metallurgical zinc leaching residue and recovery of valuable metals, International Journal of Minerals, Metallurgy and Materials, 24 (11) (2017) 1217-1227. http://doi.org/10.1007/s12613-017-1514-2.

[11] L. Cao, Y. L Liao, G. C. Shi, Y. Zhang, and M.Y. Guo, Leaching behavior of zinc and copper from zinc refinery residue and filtration performance of pulp under the hydrothermal process, International Journal of Minerals, Metallurgy and Materials, 26 (1) (2019) 21-32. http://doi.org/10.1007/s12613-019-1706-z.

[12] H. S. Han, W. Sun, Y. H. Hu, B. L. Jia, H. H. Tang, Anglesite and silver recovery from jarosite residues through roasting and sulfidization-flotation in zinc hydrometallurgy, Journal of Hazardous Materials, 278 (2014) 49-54. http://doi.org/10.1016/j.jhazmat.2014.05.091.

[13] G. Q. Liu, D. A. Pan, Y. F. Wu, H. R. Yuan, L. Yu, W. Wang, An integrated and sustainable hydrometallurgical process for enrichment of precious metals and selective separation of copper, zinc, and lead from a roasted sand, Waste Management, 132 (2021), 133-141. http://doi.org/10.1016/j.wasman.2021.07.020.

[14] G. H. Wang, Y. Cui, Ze Yang, Z. L. Guo, L. Zhao, X. M. Li, J. X. Zhao, W. D. Tang, Volatilization characteristics of high-lead slag and its influence on measurement of physicochemical properties at high temperature, Journal of Mining and Metallurgy, Section B: Metallurgy, 56 (1) (2020) 59-68. http://doi.org/10.2298/JMMB190219003W.

[15] Y. T. Ma, P. Yang, B. G Lu, Y. L. Dou, J. K. Tian, W. B. Guo, Z. Q. Zhang, Y. Y. Shen, Effect of FeO content on melting characteristics and structure of nickel slag, Journal of Mining and Metallurgy, Section B: Metallurgy, 58 (3) (2022) 427-438. http://doi.org/10.2298/JMMB220317024M.

[16] C. C. Yang, D. Q. Zhu, J. Pan, S. W. Li, H. Y. Tian, A novel process for Fe recovery and Zn, Pb removal from a low-grade pyrite cinder with high Zn and Pb contents, International Journal of Minerals, Metallurgy and Materials, 25 (9) (2018) 981-989. http://doi.org/10.1007/s12613-018-1648-x.

[17] Y. X. Zheng, J. L. Ning, W. Liu, P. J. Hu, J. F. Lü, J. Pang, Reaction behaviors of Pb and Zn sulfates during reduction roasting of Zn leaching residue and flotation of artificial sulfide minerals, International Journal of Minerals, Metallurgy and Materials, 28 (3) (2021) 358-366. http://doi.org/10.1007/s12613-020-2029-9.

[18] S. J. Lu, J. Li, D. L. Chen, W. Sun, J. Zhang, Y. Yang, A novel process for silver enrichment from Kaldo smelting slag of copper anode slime by reduction smelting and vacuum metallurgy, Journal of Cleaner Production, 261 (10) (2020) 121214. http://doi.org/10.1016/j.jclepro.2020.121214.

[19] Z. Y. Zhao, J. X. Zhao, Y. Cui, L. Lu, G. H. Wang, The influence of the volatiles on the slag composition for the heating process, Journal of Mining and Metallurgy, Section B: Metallurgy, 56 (1) (2020) 51-57. http://doi.org/10.2298/JMMB190509046Z.

[20] K. Ouyang, Z. H. Dou, T. A. Zhang, Y. Liu, L. P. Niu, Desulfurization kinetics of high lead and zinc sulfide containing slag with oxygen blowing, Journal of Mining and Metallurgy, Section B: Metallurgy, 55 (2) B (2019) 187-196. http://doi.org/10.2298/JMMB190121026Y.

[21] Y. Y. Wang, H. F. Yang, B. Jiang, R. L. Song, W. H. Zhang, Comprehensive recovery of lead, zinc, and iron from hazardous jarosite residues using direct reduction followed by magnetic separation, International Journal of Minerals, Metallurgy and Materials, 25 (2) (2018) 123-130. http://doi.org/10.1007/s12613-018-1555-1.

[22] Y. L. Li, J. Li, Y. L. Li, Y. S. Niu, X. Y. Yao, Y. B. Chen, X. W. Lu, Experimental study on volatilization of lead and zinc by reduction roasting of lead-silver slag in zinc smelting, Hydrometallurgy of China, 39 (3) (2020) 186-189. (In Chinese) http://doi.org/10.13355/j.cnki.sfyj.2020.03.003.

[23] C. Q. Xu, P. F. Xin, L. Xu, Synergistic treatment process of lead-silver slag and lead concentrate in zinc smelting, China Nonferrous Metallurgy, 51 (4) (2022) 37-42. http://doi.org/10.19612/j.cnki.cn11-5066/tf.2022.04.006.

[24] S. Y. Wu, J. Zhang, R. F. Zhao, Z. W. Ma, S. Wang, S. Q. Zhang, Research progress on environmentally friendly and efficient recovery of rare and precious metals from lead-silver slag, Gansu Metallurgy, 42 (04) (2020) 51-14. https://doi.org/10.16042/j.cnki.cn62-1053/tf.2020.04.016.

[25] H. J. Wang, Z. Y. Liu, Z. H. Liu, Y. H. Li, S. W. Li, W.

H. Zhang, Q. H. Li, Leaching of iron concentrate separated from kiln slag in zinc hydrometallurgy with hydrochloric acid and its mechanism, Transactions of Nonferrous Metals Society of China, 27(4) (2017) 901-907. https://doi.org/10.1016/S1003-6326(17)60104-3.

[26] G. D. Li, H. Lin, Y. B. Dong, X. Wang, Y. Zhang, Experimental study on asynchronous recovery of zinc and lead-silver from lead-silver slag by hydrometallurgy, Chinese Journal of Rare Metals, 41 (10) (2017) 1143-1150. https://doi.org/10.13373/j.cnki.cjrm.xy16050009.

[27] L. Tang, C. B. Tang, J. Xiao, P. Zeng, M. T. Tang, A cleaner process for valuable metals recovery from hydrometallurgical zinc residue, Journal of Cleaner Production, 201 (2018) 764-773. http://doi.org/10.1016/j.jclepro.2018.08.096.

[28] H. Stephen, Applying ausmelt technology to recover Cu, Ni, and Co from slags, JOM, 52 (8) (2000) 30-33. http://doi.org/10.1007/s11837-000-0170-5.

[29] D. K. Aliakbar, G. Ahad, Utilization of response surface methodology, kinetic and thermodynamic studies on cadmium adsorption from aqueous solution by steel slag, Journal of the Iranian Chemical Society, 18 (11) (2021) 3031-3045. http://doi.org/10.1007/s13738-021-02248-2.

POSTOJEĆE STANJE I STOPA UKLANJANJA SREBRA IZ ŠLJAKE KOJA SADRŽI OLOVO I SREBRO TOKOM PROCESA TOPLJENJA I ISPARAVANJA

Y.-Y. Shen [a], X.-S. Zhao [a], F.-J. Zhang [a], W.-X. Ma [a], X.-F. Wang [b], X.-Y. Du [a,*]

[a] Fakultet za nauku i materijale, Glavna državna laboratorija za naprednu obradu i reciklažu nefero metala, Univerzitet tehnologije u Landžou, Landžou, Narodna Republika Kina

[b] Gansu d.o.o., Baiyin, Narodna Republika Kina

Apstrakt

U ovom radu, srebro sadržano u šljaci koja sadrži olovo i srebro dobijeno je tokom procesa topljenja i isparavanja. Analizirano je postojeće stanje srebra u dimu, proučavan je uticaj temperature reakcije, odnosa ugljenika i vremena reakcije na stopu uklanjanja srebra, a procesni uslovi su optimizovani primenom metodologije odziva površine. Hlorid srebra, srebro metal, sulfid srebra, oksid srebra i sulfat srebra su glavne faze srebra u šljaci koja sadrži olovo i srebro, od kojih su hlorid srebra i sulfid srebra glavne faze. Oksid srebra (Ag_2O) i hlorid srebra (AgCl) u šljaci koja sadrži olovo i srebro isparavaju u dim, sulfid srebra (Ag_2S) se oksiduje kiseonikom u srebro-sulfat (Ag_2SO_4), a elementarno srebro isparava sa Pb i Zn kako bi formirali legure. Srebro se na kraju pojavljuje kao Ag, AgCl, Ag_2O i Ag_2SO_4 u dimu. Stopa uklanjanja srebra postepeno raste sa povećanjem temperature reakcije i tendencijom stabilizacije na 1300 °C. Sa postepenim povećanjem sadržaja ugljenika, stopa uklanjanja srebra prvo raste, a zatim opada. Najviša vrednost je 80.12 wt.% kada je sadržaj ugljenika 16.30%. Kako vreme zadržavanja raste, stopa uklanjanja srebra postepeno raste i zatim se stabilizuje na 79.97% čak i pri vremenu zadržavanja od 150 minuta. Optimalni uslovi procesa za uklanjanje srebra su temperatura reakcije od 1340 °C, sadržaj ugljenika od 16.10%, i vreme zadržavanja od 165 minuta. Prosečna stopa uklanjanja srebra pod ovim uslovima je 80.42%. Istraživanje u ovom članku pruža teorijsku osnovu za uklanjanje i iskorišćavanje srebra iz ostataka olova i srebra.

Ključne reči: *Šljaka koja sadrži olovo i srebro; Proces topljenja i isparavanja; Faze srebra; Metod odziva površine; Stopa uklanjanja*